

# Two-photon transitions driven by a combination of diode and femtosecond lasers

Marco P. Moreno,<sup>1</sup> Giovana T. Nogueira,<sup>2</sup> Daniel Felinto,<sup>1</sup> and Sandra S. Vianna<sup>1,\*</sup>

<sup>1</sup>*Departamento de Física, Universidade Federal de Pernambuco, Recife, PE 50670-901, Brazil*

<sup>2</sup>*Departamento de Física, Universidade Federal de Juiz de Fora, Juiz de Fora, MG 36036-330, Brazil*

\*Corresponding author: vianna@ufpe.br

Received July 18, 2012; revised August 27, 2012; accepted September 12, 2012;  
posted September 13, 2012 (Doc. ID 172761); published October 15, 2012

We report on the combined action of a cw diode laser and a train of ultrashort pulses when each of them drives one step of the  $5S$ - $5P$ - $5D$  two-photon transition in rubidium vapor. The fluorescence from the  $6P_{3/2}$  state is detected for a fixed repetition rate of the femtosecond laser while the cw-laser frequency is scanned over the rubidium  $D_2$  lines. This scheme allows for a velocity selective spectroscopy in a large spectral range including the  $5D_{3/2}$  and  $5D_{5/2}$  states. The results are well described in a simplified frequency domain picture, considering the interaction of each velocity group with the cw laser and a single mode of the frequency comb. © 2012 Optical Society of America  
OCIS codes: 020.1670, 020.4180.

In recent years, advances in ultrafast lasers and related optical technologies have enhanced the ability to control the interaction between light and matter [1]. In particular, the application of mode-locked lasers for high-resolution precision spectroscopy has been explored using fully stabilized optical frequency combs [2], as a direct probe of atomic transitions [3]. By incorporating pulse shaping technology, a precise control of molecular dynamics has also been demonstrated [4].

For experiments along these lines focused on two-photon transitions, a cooled and trapped sample is usually employed, such that only one group of atoms is investigated as the fs laser repetition rate is scanned [4,5]. For atomic systems with considerable Doppler broadening, excitations to different states have been isolated by applying narrowband interference filters in the exciting-lasers pathways [6,7]. In this context, the introduction of a second, cw laser opens new directions of investigation, with the narrowband laser assuming the role of a velocity-selective filter. In the case of one-photon transitions, velocity-selective spectroscopy has already been performed [8], and distinction between different hyperfine levels within the Doppler profile has been demonstrated [9].

In this Letter, the scheme with a second, cw laser is applied to investigate two-photon transitions, achieving considerably improved spectral resolution when compared to the previously reported works on velocity-selective spectroscopy with frequency combs [8,9]. We employ a diode laser and a 1 GHz Ti:sapphire laser to excite each step of the  $5S$ - $5P$ - $5D$  two-photon transition in a rubidium vapor (Fig. 1). The fluorescence of the  $6P_{3/2}$  state is detected for a fixed repetition rate of the femtosecond (fs) laser as a function of the diode frequency. This scheme allows us to perform a velocity-selective spectroscopy and investigate, simultaneously, the hyperfine levels  $5D_{3/2}$  and  $5D_{5/2}$ . Under the high repetition rate of the fs laser, the necessary condition for the accumulation of population and coherence is easily fulfilled, and a good description of the results is obtained considering a three-level cascade system interacting with two cw lasers.

A simplified scheme of the experimental setup together with the relevant energy levels is presented in

Fig. 1. A diode laser, stabilized in temperature and with a linewidth of about 1 MHz, is used to excite the  $5S_{1/2} \rightarrow 5P_{3/2}$  transition at 780 nm. A train of fs pulses generated by a mode-locked Ti:sapphire laser (BR Labs Ltda) can excite both  $5S_{1/2} \rightarrow 5P_{3/2}$  and  $5P_{3/2} \rightarrow 5D$  transitions. The two beams are overlapped, with orthogonal linear polarizations and in a counter propagating configuration, in the center of a sealed Rb vapor cell. The vapor cell is heated to  $\approx 80^\circ\text{C}$  and contains both  $^{85}\text{Rb}$  and  $^{87}\text{Rb}$  isotopes in their natural abundances.

The Ti:sapphire laser produces 100 fs pulses, with 300 mW of average power and a bandwidth of 20 nm, corresponding to  $\approx 10^4$  modes. The  $f_R = 1$  GHz repetition rate is measured with a photodiode and phase locked to a signal generator (E8663B-Agilent), with 1 Hz resolution, while the carrier-envelope-offset frequency,  $f_0$ , is left free. The diode laser can sweep over 10 GHz by tuning its injection current, and a saturated absorption setup is used to calibrate its frequency. A direct detection of the diode-beam transmission after passing through the cell gives information about the absorption in the  $5S \rightarrow 5P$  transition.

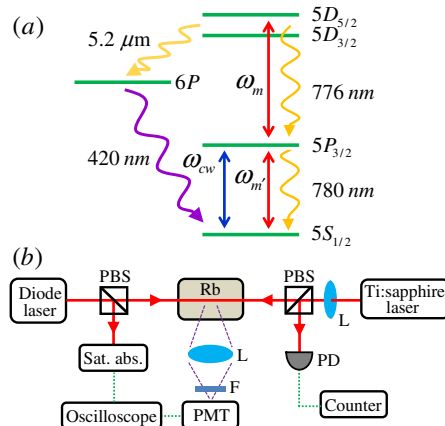


Fig. 1. (Color online) (a) Schematic representation of the energy levels of Rb, where  $\omega_{cw}$  represents the diode frequency and  $\omega_m$  and  $\omega_{m'}$  are two distinct modes of the frequency comb. (b) Experimental setup. The components are the following: PBS, polarizing beam splitter (rejection rate  $> 10^3$ ); PMT, photomultiplier tube; PD, photodetector; L, lens; F, filter.

The fluorescence at 420 nm emitted by spontaneous decay from  $6P$  state to  $5S$  is collected at  $90^\circ$ , using a 10 cm focal lens and a filter to cut the scattered light from the excitation laser beams. The signal is detected with a photomultiplier tube and recorded on a digital oscilloscope. Figure 2 shows the fluorescence signal (lower curve), for a fixed  $f_R$ , as the diode frequency is scanned over the four Doppler-broadened  $D_2$  lines of the  $^{85}\text{Rb}$  and  $^{87}\text{Rb}$ . The spectrum consists of several narrow peaks over a flat background. The narrow peaks are due to the two-photon transition excited by both lasers—the diode laser and the different modes of the frequency comb; while the background is due only to excitation by the frequency comb. In the same scan, we can observe, simultaneously, peaks associated to the excitation of the  $5D_{3/2}$  and  $5D_{5/2}$  states. We also see two peaks, separated by one  $f_R$  in optical frequency of the diode laser, that correspond to the same transition excited by two neighboring modes of the frequency comb. The saturated absorption curve (upper curve) is used to calibrate the diode frequency.

The fluorescence for the Doppler lines  $F = 2$  of  $^{87}\text{Rb}$  and  $F = 3$  of  $^{85}\text{Rb}$ , as a function of the diode frequency, is shown in Fig. 3, for a slow scan in a shorter range of frequency and a different  $f_R$  value. We also present a measurement of the direct transmission of the diode beam after passing through the warm cell (blue curve), indicating the strong absorption in the center of the Doppler lines. Figures 3(b) and 3(c) display a zoom of the two frequency regions selected in Fig. 3(a). As we can see, each peak in Fig. 2 consists of a group of peaks, which are the result of excitation from a given ground-state hyperfine level to all the hyperfine levels ( $F''$ ) of the excited state. To identify each line in Fig. 3 we use the two-photon resonance condition, combined with the position of the peak in the Doppler profile (which determines the velocity of the atoms that are resonant with both lasers) and the repetition frequency of the fs laser. Each line is the contribution of excitation through various hyperfine levels ( $F'$ ) of the intermediate state [10].

We can understand and calculate such spectra using a simple model consisting of independent three-level cascade systems interacting with two cw lasers. As we are interested in the combined action of the diode and the fs lasers, we will neglect the background. We denote one of

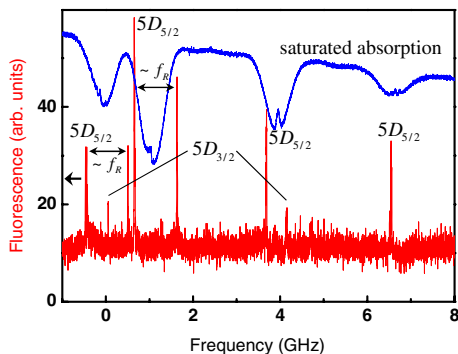


Fig. 2. (Color online) Fluorescence from the  $6P_{3/2} \rightarrow 5S_{1/2}$  decay as a function of the diode laser frequency for the four  $D_2$  Doppler lines. The saturated absorption signal (upper curve) is detected simultaneously.

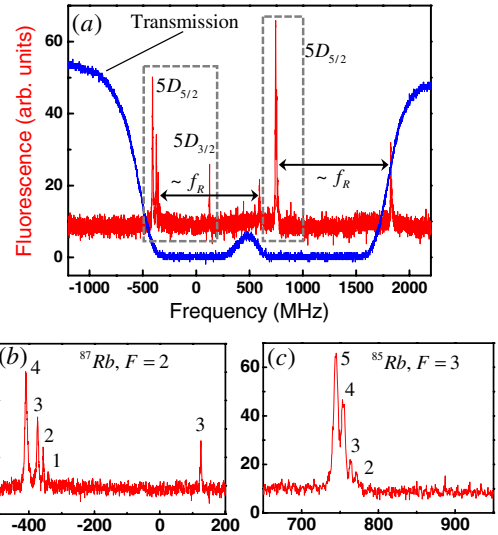


Fig. 3. (Color online) (a) Fluorescence at 420 nm as a function of the diode laser frequency. The diode transmission after the Rb cell (blue curve) is detected simultaneously. Zooms of the regions inside the two rectangles in (a) for excitation from the hyperfine ground states, (b)  $F = 2$  of  $^{87}\text{Rb}$ , and (c)  $F = 3$  of  $^{85}\text{Rb}$ . The numbers at the peaks denote the hyperfine final state of the transition.

the hyperfine levels of the ground ( $5S_{1/2}, F'$ ), intermediate ( $5P_{3/2}, F''$ ), and final ( $5D, F'''$ ) states as  $|1\rangle$ ,  $|2\rangle$ , and  $|3\rangle$ , respectively. The train of ultrashort pulses is described in the frequency domain as a frequency comb and we take into account only the modes that are near resonance with the  $|2\rangle \rightarrow |3\rangle$  transitions. We also consider that the transitions  $|1\rangle \rightarrow |2\rangle$  are only driven by the diode laser. As the diode beam may be intense, we cannot apply second-order time-dependent perturbation theory, as in [6]. The calculations are performed from the full Bloch equations for a three-level cascade system. The  $|1\rangle \rightarrow |2\rangle$  transitions may be open or closed, depending on which  $F''$  is being excited. However, due to the longer lifetimes of the  $5D$  states (resulting in weaker optical pumping) and to simplify the calculations, we consider that the  $|2\rangle \rightarrow |3\rangle$  transitions are always closed.

For a specific transition  $F \rightarrow F'' \rightarrow F'''$ , we calculate the population  $\rho_{33}$  of the final  $F'''$  state in the steady-state regime by solving the Bloch equation for one specific diode frequency ( $\delta$ ) integrated over the contribution of all velocity groups ( $\Delta$ ) within the Doppler profile:

$$\rho_{33}^{(F, F'', F''')}(\delta) = \int_{-\infty}^{\infty} \frac{\rho_{33}(\Delta, \delta)}{\sqrt{\pi}0.6\Delta_D} e^{-(\Delta/0.6\Delta_D)^2} d\Delta, \quad (1)$$

with  $\Delta_D$  being the inhomogeneous Doppler linewidth. In the calculations, the strength of a specific  $F_i \rightarrow F_j$  transition is parametrized by the corresponding Rabi frequency:  $\Omega_{F_i, F_j} = (\mu_{F_i, F_j} E)/\hbar$ , where  $\mu_{F_i, F_j}$  is the electric-dipole moment for the transition and in the direction of the electric field, whose amplitude  $E$  may refer to the diode laser or a single mode of the frequency comb, depending on the transition.

To compare with the experimental spectra, we need to add the contributions due to all allowed two-photon transitions:  $\rho_{33}^{\text{calc}}(\delta) = \sum_{F, F'', F'''} \rho_{33}^{(F, F'', F''')}(\delta)$ . We consider that

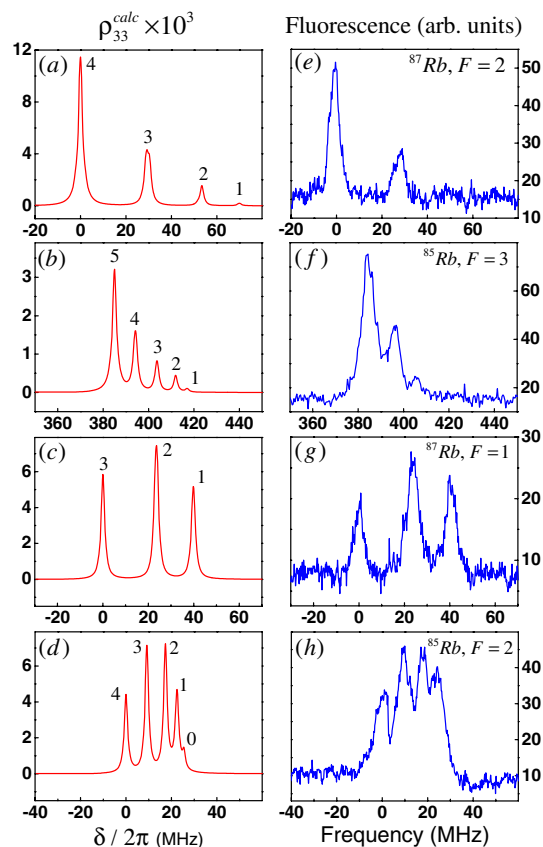


Fig. 4. (Color online) (a)–(d) Calculated population of level  $|3\rangle$ ,  $\rho_{33}^{\text{calc}}(\delta)$ , and (e)–(h) experimental results for the fluorescence at 420 nm, as a function of the diode frequency, for the four  $D_2$  Doppler lines.

the two beams have orthogonal polarizations and sum all contributions weighted by the corresponding electric-dipole moments. We also take into account that more than one velocity group contributes to the fluorescence from each two-photon transition [6,10]. Figure 4 shows the calculated population  $\rho_{33}^{\text{calc}}(\delta)$  of level  $|3\rangle$  for four different groups of peaks at each of the  $D_2$  Doppler lines. At the right column of Fig. 4 we display the experimental results obtained for the same conditions used in the calculations. As we can see, a good description of the experimental results is obtained, although the peaks appear wider than the calculated ones. We attribute

the larger widths of the experimental peaks mainly to the linewidth of the diode laser itself, the jitter of the off-set frequency, and contributions of the magnetic field broadening.

In conclusion, we show that the combined action of a cw laser and a train of ultrashort pulses can be used to drive two-photon transitions efficiently and with high spectral resolution. Although the experimental resolution is limited by the free-running offset frequency and the linewidth of the diode laser, we are able to investigate simultaneously a large spectral range including the  $5D_{3/2}$  and  $5D_{5/2}$  states with good spectral resolution, and without the need of direct spectral filtering of the fs laser. A direct, quantitative description of the experimental spectra is given in the frequency domain picture, highlighting all physical elements that are important to explain our results.

This work was supported by CNPq, FACEPE, and CAPES (Brazilian Agencies).

## References

1. J. Ye and S. T. Cundiff, *Femtosecond Optical Frequency Comb Technology: Principle, Operation and Application* (Springer, 2005).
2. D. J. Jones, S. A. Diddams, J. K. Ranka, A. Stentz, R. S. Windeler, J. L. Hall, and S. T. Cundiff, *Science* **288**, 635 (2000).
3. M. C. Stowe, M. J. Thorpe, A. Pe'er, J. Ye, J. E. Stalnaker, V. Gerginov, and S. A. Diddams, *Adv. At. Mol. Opt. Phys.* **55**, 1 (2008).
4. M. C. Stowe, A. Pe'er, and J. Ye, *Phys. Rev. Lett.* **100**, 203001 (2008).
5. A. Marian, M. Stowe, J. Lawall, D. Felinto, and J. Ye, *Science* **306**, 2063 (2004).
6. J. E. Stalnaker, V. Mbele, V. Gerginov, T. M. Fortier, S. A. Diddams, L. Hollberg, and C. E. Tanner, *Phys. Rev. A* **81**, 043840 (2010).
7. J. E. Stalnaker, S. L. Chen, M. E. Rowan, K. Nguyen, T. Pradhananga, C. A. Palm, and D. F. J. Kimball, "Velocity-selective direct frequency-comb spectroscopy of atomic vapors," <http://www.arxiv.org/physics.atom-ph/arXiv:1206.0999v1>.
8. D. Aumiler, T. Ban, H. Skenderović, and G. Pichler, *Phys. Rev. Lett.* **95**, 233001 (2005).
9. M. P. Moreno and S. S. Vianna, *J. Opt. Soc. Am. B* **28**, 2066 (2011).
10. J. E. Bjorkholm and P. F. Liao, *Phys. Rev. A* **14**, 751 (1976).